Calculated Phonon Spectra of Plutonium at High Temperatures

X. Dai,[1] S. Y. Savrasov,[2]* G. Kotliar,[1] A. Migliori,[3] H. Ledbetter,[3] E. Abrahams[1]

We constructed computer-based simulations of the lattice dynamical properties of plutonium using an electronic structure method, which incorporates correlation effects among the f-shell electrons and calculates phonon spectra at arbitrary wavelengths. Our predicted spectrum for the face-centered cubic δ phase agrees well with experiments in the elastic limit and explains unusually large shear anisotropy of this material. The spectrum of the body-centered cubic phase shows an instability at zero temperature over a broad region of the wave vectors, indicating that this phase is highly anharmonic and can be stabilized at high temperatures by its phonon entropy.

Plutonium (Pu) is a material with very unusual solid-state properties. Despite its scientific and technological importance, many of its key properties, such as the spectrum of lattice vibrations, remain uninvestigated. It has not been possible to measure that spectrum experimentally because of Pu's extreme toxicity and radioactivity. It has not been possible to compute the spectrum theoretically, because Pu is strongly correlated, and the traditional electronic structure methods fail to describe it even qualitatively. These studies are, however, essential to be able to address the factors that govern the lattice stability of Pu, an issue that is important for Pu's storage and disposal over long time scales.

Pu has six crystallographic allotropes with puzzling volume variations among them (1). Starting from the low-temperature α structure with 16 atoms in the elementary cell, it undergoes a series of phase transitions ending in relatively simple face-centered cubic (fcc) (δ) and body-centered cubic (bcc) (ε) phases at temperatures greater than 500 K. The 25% volume increase during the transition from α to δ is followed by a volume contraction upon further heating (2) through the δ-ε transition, occurring by way of an intermediate body center tetragonal δ' phase, which exists in a very narrow temperature interval. It is the unusual behavior of both the electronic and lattice degrees of freedom that determines the rich phase diagram of Pu.

The experimental information about the lattice dynamical properties of this element is very limited. Pu has relatively soft elastic constants and a Debye temperature near 100 K (3). Using this information, phenomenological studies of the thermodynamics of Pu have been carried out (4). However, the role phonons play in the thermodynamics of Pu is unclear because of the lack of appropriate theoretical and experimental tools to study its lattice-dynamical properties. We address this issue based on a new approach that is capable of microscopically calculating phonons in strongly correlated systems.

Our method is based on a recently developed (5) electronic structure algorithm, which allows us to include dynamical self-energy effects in calculating total energies and spectra of materials with correlated electrons. Its foundation is provided by the dynamical mean field theory (DMFT) (6), which treats systems with competing localization and delocalization tendencies of the electrons, where such methods as the density functional theory (7) in its local density approximation (LDA) or generalized gradient approximations (GGAs) have limited applicability. For example, within the LDA, the theoretical volumes of δ Pu and ε Pu are 30% too small, the bulk modulus is one order of magnitude too large, and long-range magnetic order is predicted that is not experimentally observed (8–12). Many of these difficulties have been corrected by using DMFT-based calculations (5).

The approach we used to compute the phonon spectrum of strongly correlated systems combines DMFT and linear response theory. It can be used to study the vibrations that involve arbitrary wave vectors of atomic displacements (13). A perturbative method with respect to small movements of atoms from their equilibrium positions is used to evaluate changes in the electronic charge densities, potentials, local Green functions, and self-energies caused by

lattice vibrations. The dynamical matrix is evaluated as the second-order derivative of the expression for the total energy within DMFT (14). This provides important information about how electronic correlations affect the lattice vibrations.

Why are lattice dynamics studies required for understanding the phases of Pu? Here, the f-shell electrons are close to the Mott transition (15). The compressibility at a Mott transition end point diverges (16), which suggests anomalous elastic properties in its vicinity. In isostructural phase transitions such as the α-γ transition in cerium (17, 18), the entropy changes associated with the lattice deformations can be safely neglected. In Pu, however, these entropy changes can be large.

Because Pu does not show long-range magnetic order, magnetic moments on Pu atoms can exist only locally. Therefore, only dynamical self-energy effects can describe the notion of the disordered local moments. They can be treated using the DMFT on the level of the so-called Hubbard I approximation (19) for the Anderson impurity model (20), which describes the Pu's paramagnetic state.

We calculated total energies of fcc and bcc structures of Pu as a function of volume using a self-consistent dynamical mean field method. We solved the impurity model within various schemes ranging from simple Hartree-Fock–like magnetically ordered LDA+U (where U is the total energy) (21, 22) to paramagnetic Hubbard-I and more sophisticated iterative perturbation theory–based interpolation methods (5, 6). We used $U = 4$ eV in our simulations as approximately given by the atomic spectral data (23), constrained density functional studies (24), and our previous work (5, 21). All techniques gave us a good agreement in predicting the equilibrium volumes for δ Pu and ε Pu: V_δ was obtained to be 15.9 cm³/mol, which is only 6% larger than the experiment in (2), and the ε-phase volume is predicted to be 3% smaller than V_δ, in accordance with the experiment in (2). The emerging physical picture indicates an ε phase that has slightly more itinerant electrons than the δ phase. Why then does the more itinerant phase, with its smaller volume, become favorable at higher temperatures? The answer lies in the spectrum of vibrations of these two phases.

We calculated the phonon spectra in δ and ε Pu by using the linear response technique (13, 25). Self-energy effects in the calculation of the dynamical matrix were included, using the Hubbard-I approximation (19). In the calculated frequencies, as a function of wave vector along high-symmetry directions in the Brillouin zone for the δ phase (Fig. 1), we saw a considerable softening of the transverse

[1]Department of Physics and Astronomy and Center for Materials Theory, Rutgers University, Piscataway, NJ 08854, USA. [2]Department of Physics, New Jersey Institute of Technology, Newark, NJ 07102, USA. [3]Los Alamos National Laboratory, Los Alamos, NM 87545, USA.

*To whom correspondence should be addressed. E-mail: savrasov@oak.njit.edu

phonons around the L point, indicating that the δ phase may be close to an instability with a doubling of the unit cell. Another anomaly is seen for the transverse acoustic mode along (011), which is connected to the nonlinear behavior of the lowest branch at small q values. Overall, the phonon frequencies are positive, showing the internal stability of the positions of the nuclear coordinates in δ Pu.

Using our calculated dispersion relations $\omega(q)$, we extracted the elastic constants of δ Pu. For a cubic crystal, these are reduced to three independent parameters: C_{11}, C_{44}, and C_{12}, which can be found from the estimates of the corresponding sound velocities $d\omega/dq$ along (100) and (110). The relationships for the longitudinal and the transverse sound along (100) are $V_1 = (C_{11}/\rho)^{1/2}$, $V_t = (C_{44}/\rho)^{1/2}$, where ρ is the density of the material. C_{12}, as well as another frequently used constant, C', involve combinations of C_{11}, C_{44}, and the sound velocities along (110). We compared the results of our calculations with the experimental data in (26) (Table 1).

We saw several unusual features in the elastic behavior. First, C_{11} was very close to C_{44}, which gave nearly coinciding longitudinal and transverse acoustic phonons along (001). A similar conclusion can be drawn from Fig. 1, in which two phonon branches along this direction are nearly degenerate at small q values. In ordinary metals, the C_{11}:C_{44} ratio is often much larger than 1. Second, the deviation from the Cauchy relation, $C_{44} = C_{12}$, which measures the importance of the angular dependence in atomic forces as compared to the central force description, was very small. Third, the distortion described by $C' = (C_{11} - C_{12})/2$ is very 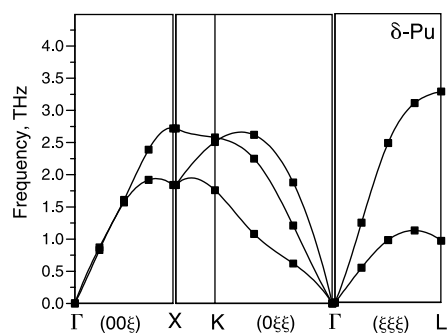soft, nearly like a liquid, which highlights a huge anisotropy in elastic properties of δ Pu along different directions. C' measures the rigidity against the volume-conserving tetragonal deformation. This is in fact the deformation from fcc (δ) toward a bcc (ε) lattice along a path known as the Bain path. Previous (10) LDA+U and our Hubbard-I–based studies show that the total energy difference between the δ and ε phases is quite small and by order of magnitude is close to 1000 K. It is therefore reasonable to expect soft behavior along the Bain path. This can also shed light on the negative volume thermal expansion, which is another puzzle in δ Pu. Because of small energy variation along the Bain path, the fcc lattice can fluctuate toward the bcc structure, which has a lower volume.

The results in Table 1 agree well with the measured data (26), which indicates that our method of determining the lattice dynamics in this strongly correlated metal is quite accurate. The LDA+U–based calculations that assume the existence of long-range magnetic order also give the elastic constants in much better agreement with experiments than LDA alone, although residual discrepancies on the order of 50% remain (10). The present result shows a substantial improvement, mainly because of nearly coinciding longitudinal and transverse sounds along (001), in accordance with the measurements.

We now turn to the description of our results for the phonon dispersions of ε Pu (Fig. 2). In the ε phase, we find several modes that are totally unstable at zero temperature (T). First, the transverse phonon branch along (011) with the polarization vector [0, 1, –1] is unstable for all values of q. Second, the transverse branch along (011) with the polarization vector [1, 0, 0] is unstable at large values of q. We also noticed a large, nearly unstable softening of both longitudinal and transverse phonon modes near the H point. This is very different from the internally stable dynamics of the Pu nuclei in the δ phase. How can we understand the mere existence of ε Pu if our $T = 0$ calculations predict it to be unstable? The key lies in anharmonicity and finite temperature phonon entropy.

Applying the frozen phonon method to the most unstable anharmonic mode at [0, π, π], we obtain a double-well potential, as shown in the inset of Fig. 2. The depth of the double well is about 1500 K, which is comparable to the temperatures 750 to 900 K, at which the ε phase is found to be stable. The vibrations in this phase are extremely anharmonic and involve large nuclei excursions from their equilibrium positions. This results in the soft phonon spectrum, which is only stable at high temperatures. The latter conclusion is also confirmed by the analysis of the thermodynamics of Pu (4), from which the Debye frequency for the ε phase is extracted to be only 63 K as compared with the corresponding value of 92 K for the δ phase. A slightly higher value of 110 K has recently been obtained (27) for δ Pu by the extended x-ray absorption fine structure technique.

We are now ready to shed new light on the thermodynamics of the δ-to-ε phase transition, stressing the importance of the phonon entropy. The free energy difference $\Delta F = F_\varepsilon(T) - F_\delta(T)$ between these phases is described by both lattice and electronic degrees of freedom and includes both U and the entropy (TS) terms: $F = U - TS$. Unfortunately, accurately evaluating each of these contributions is not a straightforward task. For the phonon part, even for weakly correlated materials, extreme anharmonic situations pose substantial computational and conceptual challenges (28). Accurate evaluation of electronic entropies is another problem. In spite of these difficulties, several conclusions are very robust. Our total energy Hubbard-I–based calculations place the smaller volume ε phase higher in energy than δ by 700 K. We used the method of (28), which decouples different modes in q space and interpolates the double wells as functions of q, to demonstrate that the anharmonic terms in the phonon free energy favor ε over δ by an amount approximately equal to 1000 K. This magnitude is sufficient to compensate for the electronic energy loss in going from δ to the slightly smaller volume ε phase.

Thus, we obtain a new insight into the volume contraction between δ and ε phases that Pu undergoes upon heating. Both high-temperature phases are strongly correlated with a very similar electronic structure; ε has a slightly higher electronic energy and slightly more itinerant electronic f states than δ.

Fig. 1. Calculated phonon dispersion relations for δ Pu using the dynamical mean field linear response method. Γ = (0, 0, 0) $2\pi/a$; X = (0, 0, 1) $2\pi/a$; K = (0, 3/4, 3/4) $2\pi/a$; L = (1/2, 1/2, 1/2) $2\pi/a$, where a is the lattice constant for δ-Pu.

Table 1. Comparison between calculated and experimental (26) elastic constants in δ Pu.

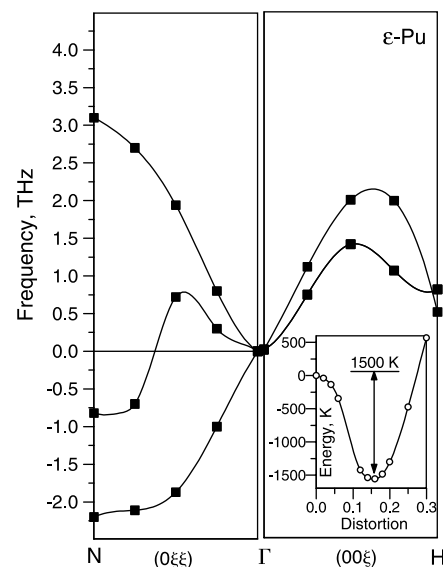|	C_{11} (GPa)	C_{44} (GPa)	C_{12} (GPa)	C' (GPa)
Theory	34.56	33.03	26.81	3.88
Experiment	36.28	33.59	26.73	4.78

Fig. 2. Calculated phonon dispersion relations for ε Pu using the dynamical mean field linear response method. The inset shows total energy (K) as a function of distortion (in units of lattice constant) for the most unstable transverse branch at the N point N = (0, 1/2, 1/2) $2\pi/a$; H=(0, 0, 1) $2\pi/a$, where a is the lattice constant for ε-Pu.

This results in a lower volume. The difference between the two phases lies in the phonon dynamics. Although the phonons in δ Pu are fairly harmonic, our calculation reveals substantial instability in several modes of ε Pu. This anharmonicity results in a much higher phonon entropy, which in turn stabilizes the ε-Pu phase at high temperatures.

References and Notes

1. For a review, see A. J. Freeman, J. B. Darby, Eds., *The Actinides: Electronic Structure and Related Properties* (Academic Press, New York, 1974), vols. 1 and 2.
2. S. S. Hecker, L. F. Timofeeva, *Los Alamos Sci.* **26**, 244 (2000).
3. A. Migliori, J. Baiardo, L. T. Darling, *Los Alamos Sci.* **26**, 208 (2000).
4. D. C. Wallace, *Phys. Rev. B* **58**, 15433 (1998).
5. S. Y. Savrasov, G. Kotliar, E. Abrahams, *Nature* **410**, 793 (2001).
6. For a review, see A. Georges, G. Kotliar, W. Krauth, M. J. Rozenberg, *Rev. Mod. Phys.* **68**, 13 (1996).
7. For a review, see S. Lundqvist, S. H. March, Eds., *Theory of the Inhomogeneous Electron Gas* (Plenum, New York, 1983).
8. P. Soderlind, O. Eriksson, B. Johansson, J. M. Wills, *Phys. Rev. B* **50**, 7291 (1994).
9. M. D. Jones, J. C. Boettger, R. C. Albers, D. J. Singh, *Phys. Rev. B* **61**, 4644 (2000).
10. J. Bouchet, B. Siberchicot, F. Jollet, A. Pasturel, *J. Phys. Condens. Matter* **12**, 1723 (2000).
11. H. L Skriver, O. K Andersen, B. Johansson, *Phys. Rev. Lett.* **41**, 42 (1978).
12. I. V. Solovyev, A. I. Liechtenstein, V. A. Gubanov, V. P. Antropov, O. K. Andersen, *Phys. Rev. B* **43**, 14414 (1991).
13. S. Y. Savrasov, *Phys. Rev. Lett.* **69**, 2819 (1992).
14. G. Kotliar, S. Y. Savrasov, in *New Theoretical Approaches to Strongly Correlated Systems*, A. M. Tsvelik, Ed. (Kluwer Academic, Amsterdam, 2001), pp. 259–301.
15. B. Johansson, *Philos. Mag.* **30**, 469 (1974).
16. G. Kotliar, S. Murthy, M. J. Rozenberg, *Phys. Rev. Lett.* **89**, 046401 (2002).
17. K. Held, A. K. McMahan, R. T. Scalettar, *Phys. Rev. Lett.* **87**, 276404 (2001).
18. B. Johansson, I. A. Abrikosov, M. Aldén, A. V. Ruban, H. L. Skriver, *Phys. Rev. Lett.* **74**, 2335 (1995).
19. J. Hubbard, *Proc. R. Soc. London Ser. A* **281**, 401 (1964).
20. P. W. Anderson, *Phys. Rev.* **124**, 41 (1961).
21. S. Y. Savrasov, G. Kotliar, *Phys. Rev. Lett.* **84**, 3670 (2000).
22. For a review, see V. I. Anisimov, F. Aryasetiawan, A. I. Lichtenstein, *J. Phys. Condens. Matter* **9**, 767 (1997).
23. J. P. Desclaux, A. J. Freeman, in *Handbook on the Physics and Chemistry of the Actinides*, A. J. Freeman, G. H. Lander, Eds. (Elsevier, Amsterdam, 1984), vol. 1.
24. P. E. A. Turchi, A. Gonis, N. Kioussis, D. L. Price, B. R. Cooper, in *Electron Correlations and Materials Properties*, A. Gonis, N. Kioussis, M. Ciftan, Eds. (Kluwer Academic, New York, 1999), pp. 531–537.
25. S. Y. Savrasov, G. Kotliar, *Phys. Rev. Lett.* **90**, 056401 (2003).
26. H. M. Ledbetter, R. L. Moment, *Acta Metallurgica*, **24**, 891 (1976).
27. P. G. Allen *et. al.*, *Phys. Rev. B* **65**, 214107 (2002).
28. N. D. Drummond, G. J. Ackland, *Phys. Rev. B* **65**, 184104 (2002).
29. Supported by the NSF Division of Material Research (grants 02382188 and 0096462), U.S. Department of Energy division of Basic Energy Sciences (grant DE-FG02-99ER45761), and Los Alamos National Laboratory (subcontract 44047-001-0237).

Microfluidic Memory and Control Devices

Alex Groisman,* Markus Enzelberger, Stephen R. Quake†

We demonstrate microscopic fluidic control and memory elements through the use of an aqueous viscoelastic polymer solution as a working fluid. By exploiting the fluid's non-Newtonian rheological properties, we were able to demonstrate both a flux stabilizer and a bistable flip-flop memory. These circuit elements are analogous to their solid-state electronic counterparts and could be used as components of control systems for integrated microfluidic devices. Such miniaturized fluidic circuits are insensitive to electromagnetic interference and may also find medical applications for implanted drug-delivery devices.

Fluidics, the construction of fluidic devices similar to electronic circuits, was an active field of research technology in the 1960s and early 1970s. Fluidic circuits were an alternative to vacuum tubes and solid-state electronics (*1*, *2*), and advanced fluidic devices such as oscillators, flip-flops, amplifiers, and logic gates were built and integrated into sophisticated control systems (*1*, *2*). Fluidic circuits ultimately lost the competition with semiconductor electronics in part because they could not be easily miniaturized, placing severe limits on their size and ultimate complexity. Miniaturization was not feasible because the devices are based on nonlinear inertial flow phenomena at high Reynolds numbers, *Re* (*3*). When the size is reduced, achieving sufficiently large *Re* to generate these nonlinearities requires increasingly high driving pressures and becomes impractical at the submillimeter scale.

With the advent of miniaturized plumbing and other microfluidic technologies, there is an increased need for logic and control systems to operate such devices without the use of external electronics or interfaces. Although there are some examples showing how complexity and nonlinearity can be introduced into microfluidic devices through the use of multiphase flows (*4*) or chemically responsive materials (*5*), few logic, memory, or control elements have been demonstrated. Here, we show that major nonlinear flow effects can be achieved in microfluidic devices with a single fluid and no moving parts. We demonstrate two microscale nonlinear fluidic devices that can operate at arbitrarily low *Re*: a flux stabilizer, which is analogous to an electronic constant-current source, and a bistable flip-flop, which is analogous to a digital flip-flop memory.

The nonlinearity required for the operation of these devices derives from the use of a working fluid with nonlinear mechanical properties: a viscoelastic polymer solution (*6*). The elastic properties of solutions of flexible polymers can lead to many interesting nonlinear phenomena, including purely elastic flow instabilities (*7*) and elastic turbulence (*8*). The strength of nonlinear elastic effects depends on the Weissenberg number (*5*) $Wi = \lambda \nabla V$, where ∇V is the rate of deformation in the flow and λ is the polymer relaxation time. These elastic effects are essentially independent of *Re* and should not diminish when the device is miniaturized (*6*), but such transitions have not previously been observed in microscopic flows. In this work, we found substantial transitions in microchannels even when using polymer solutions with such low viscosities and short relaxation times that viscoelastic effects would be difficult to measure in macroscopic experiments.

The flux stabilizer that we constructed is shown in Fig. 1. It is a nonlinear fluidic resistor, where the volumetric flux rate, *Q*, through a channel of a special shape depends on the applied pressure in a nonlinear fashion. The channel is a chain of halves of broad ellipsoidal rings interconnected by narrow bottlenecks (*9*), thus forcing the working fluid through a sequence of expansions and contractions (*10*). When a fluid element passes through a contraction, it becomes extended along the flow direction, as do the polymer molecules within it. If the rate of extension, $\dot{\varepsilon}$, is sufficiently large compared to $1/\lambda$, the polymer molecules can unravel (*11*). Their contribution to the flow resistance grows quickly and nonlinearly, and the apparent viscosity of the polymer solution may increase by a few orders of magnitude (*12*). Transition to this nonlinear flow regime is independent of *Re* and should occur when *Wi* is greater than 0.5 (*6*, *11*, *12*).

The dependence of *Q* on the pressure drop per segment, ΔP (*13*), is shown in Fig. 2. Ini-

Department of Applied Physics, California Institute of Technology, MS 128-95, Pasadena, CA 91125, USA.

*Present address: Department of Physics, University of California San Diego, 9500 Gilman Drive, La Jolla, CA 92093–0319, USA.
†To whom correspondence should be addressed. E-mail: quake@caltech.edu